Adiabatic Compressed Air Energy Storage with packed bed thermal energy storage

Adiabatic Compressed Air Energy Storage with Packed Bed Thermal Energy Storage

Edward Barbour[1,*], Dimitri Mignard[2], Yulong Ding[1], Yongliang Li[1,†]
[1]School of Chemical Engineering, University of Birmingham
[2]Institute for Energy Systems, University of Edinburgh

Abstract

The majority of articles on Adiabatic Compressed Air Energy Storage (A-CAES) so far have focussed on the use of indirect-contact heat exchangers and a thermal fluid in which to store the compression heat. While packed beds have been suggested, a detailed analysis of A-CAES with packed beds is lacking in the available literature. This paper presents such an analysis. We develop a numerical model of an A-CAES system with packed beds and validate it against analytical solutions. Our results suggest that an efficiency in excess of 70% should be achievable, which is higher than many of the previous estimates for A-CAES systems using indirect-contact heat exchangers. We carry out an exergy analysis for a single charge-storage-discharge cycle to see where the main losses are likely to transpire and we find that the main losses occur in the compressors and expanders (accounting for nearly 20% of the work input) rather than in the packed beds. The system is then simulated for continuous cycling and it is found that the build-up of leftover heat from previous cycles in the packed beds results in higher steady state temperature profiles of the packed beds. This leads to a small reduction (<0.5%) in efficiency for continuous operation.

Keywords

Adiabatic Compressed Air Energy Storage; Packed Beds; Thermal Energy Storage; Thermodynamic Analysis

Nomenclature

γ	ratio of specific heats of air (-)
ε	void fraction (-)
η	polytropic efficiency (-)
λ	thermal conductivity ($Wm^{-1}K^{-1}$)
μ	dynamic viscosity (Pas)
ρ	density (kgm^{-3})
τ	thickness (m)
χ	hoop stress (Pa)
ψ	shape factor (-)
A	area (m^2)
B	exergy (J)
c	specific heat capacity ($Jkg^{-1}K^{-1}$)
d	diameter (m)
G	core mass velocity ($kgm^{-2}s^{-1}$)
g	gravitational constant (ms^{-2})
h	enthalpy (J)
$\acute{h}$	heat transfer coefficient ($Wm^{-2}K^{-1}$)
$\acute{h}_{vol}$	volumetric heat transfer coefficient ($Wm^{-3}K^{-1}$)
L	Length (m)
m	mass (kg)
n	moles (mol)
p	pressure (Pa)
Q	heat (J)
R	specific molar gas constant ($Jkg^{-1}K^{-1}$)
R_{th}	thermal resistance (KW^{-1})
r	radius (m)
T	Temperature (K)
t	time (s)
V	volume (m^3)
v	velocity (ms^{-1})

W	work (J)
z	height (m)

1. Introduction

If humanity is to continue to meet its energy needs in a sustainable future, it is likely that the renewable energy era must truly come of age. Although the last 20 years has seen a considerable increase in the global installed capacity of renewable energy generation, many renewable generators are intermittent and cannot completely replace conventional thermal generation. Effective energy storage would provide one way to resolve this issue and several academic articles have been written on this topic, i.e. [1, 2]. It should be noted that in addition to energy storage, future energy systems will need a mix of demand-side management and interconnectivity [3, 4]. Several articles suggest that there may be significant benefits available from cost-effective small-scale energy storage devices; in distribution networks [5], to tidal current energy [6], and for applications in isolated island grids [7]. This article considers the construction of a 2 MWh A-CAES system with packed bed regenerators to act as the thermal stores.

Two conventional CAES plants have been in existence for more than 20 years; Huntorf, Germany (since 1978) and McIntosh, Alabama (since 1991) [8, 9]. Conventional CAES plants are hybrid air-storage/gas-combustion plants, essentially using low-cost electricity to run the compressor in a single cycle gas turbine. Typical single cycle gas turbines (peaking plants) are 35-40% efficient, so require 2.5-2.86 kWh of gas for each kWh of peak electricity produced. This can be compared to the McIntosh CAES plant which uses 0.69 kWh of off-peak electricity and 1.17 kWh of gas to produce 1 kWh of peak electricity [10]. There has been some recent work regarding coupling conventional CAES with wind energy to provide dispatchable utility-scale electricity generation [11-13].

The Adiabatic CAES (A-CAES) concept is different from conventional CAES because it functions without the combustion of natural gas, and as such does not require the availability and storage of this fossil fuel. In A-CAES surplus energy is used to power compressors which drive air into a high pressure store (this store could be artificially manufactured or be a naturally occurring cavern). The thermal energy generated by the compression is stored in Thermal Energy Stores (TES's) and then used to reheat the air before it is expanded again. To generate electricity the air is reheated and expanded through turbines which drive generators. Although, to the best of the authors' knowledge, no A-CAES plant has ever been built, it is often cited as a storage option in articles comparing energy storage technologies [14-16], usually with an expected efficiency of 70-75% [14, 16]. Recent research in A-CAES includes the ongoing EU based "Project ADELE" being undertaken by RWE Power, General Electric, Züblin and DLR, which quotes the expected efficiency at 70% [17]. Garrison and Webber [18] present a novel design for an integrated wind-solar-A-CAES system which uses solar energy to re-heat the compressed air before expansion, with an overall energy efficiency of 46%. Pimm *et al.* [19] describe a novel approach in which "bags" of compressed air are stored under the sea; the air storage is essentially isobaric as the pressure is determined by the depth. Garvey [20] presents an analysis of a large-scale integrated offshore-wind and A-CAES system using these energy bags. This approach is also being investigated by Cheung *et al*. [21] in partnership with Hydrostor [22]. Commercial companies Lightsail [23] and SustainX [24] are developing near-isothermal CAES but their technologies are yet to reach the market so details on the processes and performances are scarce.

Several articles have specifically analysed the A-CAES concept, but most consider using indirect-contact heat exchangers and a separate thermal fluid to store the compression heat. Bullough *et al*. estimates an efficiency greater than 70% [25], Grazzini and Milazzo model a 16,500MJ (~4.6MWh) system and suggest an efficiency of 72% [26], while Pickard *et al*. suggest a practical efficiency greater than 50% for a bulk A-CAES facility (1GWd) may be hard to achieve [27]. This discrepancy is not easily explained, but seems at least in part to come from Pickard *et al*. modelling the cooling stages as isochoric rather than isobaric. We suggest this is inappropriate as one purpose of cooling is to reduce the volume of the air. We also disagree with the statement in this paper that a thermal effectiveness of 0.8 imposes a ceiling of 64% upon the cycle efficiency. In A-CAES energy is stored in *both* the compression heat and the cool pressurised air – i.e. a thermal effectiveness of zero would not lead to 0% efficiency, as work would still be extractable from the compressed air. Kim *et al*. calculate an efficiency of 68% without any external heat input [28]. Grazzini and Milazzo discuss design criteria, emphasizing the importance of heat exchanger design [29]. Hartmann *et al*. [30] analyses a range of A-CAES configurations, concluding that an efficiency of 60% is realistic, however it should be noted that

the configurations mostly involve multiple compression stages and a single expansion stage. Since thermodynamic work is path dependent these systems are intrinsically inefficient; in order to minimise irreversibilities the expansion path should be a close match to the reverse of the compression path. Their analysis of a system with a single compression stage and single expansion stage highlights that a combination of a fixed temperature TES and a sliding compression (in which the outlet temperature is constantly changing) leads to a poor efficiency (~52% in their analysis). Wolf and Budt (2014) [31] suggest that with lower TES temperatures A-CAES may be more economical despite having a lower efficiency (~56%), due to quicker start-up times allowing it to participate in energy reserve markets. We believe that one aspect of previous A-CAES analyses that has been largely overlooked is the effect of (or how to avoid) mixing of thermal storage at different temperatures (when using indirect-contact heat exchangers) as the outlet temperatures of the compressors changes with the pressure of the stored air.

A related developing energy storage technology that uses thermal energy storage in packed beds is Pumped Thermal Electricity Storage (PTES). Desrues *et al*. [32] analyses a PTES system which uses electricity to pump heat between packed beds, before using a heat engine to produce electricity at a later time. White *et al*. [33] undertakes a detailed theoretical analysis of thermal front propagation in packed beds for energy storage. Although the use of packed beds for heat storage in A-CAES has been suggested, a detailed analysis of this type of system is hard to find in the literature. This article presents a thermodynamic analysis of an A-CAES system using packed bed regenerators for the TES's.

2. Thermodynamics

2.1 Compression and Expansion

Reversible isothermal compression and expansion would provide the ideal for CAES, as heat could theoretically be exchanged with the environment at ambient temperature and separate thermal energy storage would not be required. However, although there is significant research into near-isothermal compression for CAES (by companies like Lightsail and SustainX), it is not yet commercially available and any currently available compression that approaches reversible isothermal compression is too slow for industrial use [27, 28] due to the impractically small temperature differences required. Therefore most commonly cited A-CAES designs opt for a series of adiabatic or polytropic compressions, after each of which the air is cooled back to the ambient temperature in order to reduce the both the temperature and volume of the air.

The compressor work per unit mass can be estimated by considering the conservation of energy for the compressor control volume (neglecting changes in potential and kinetic energy from inlet to outlet):

$$\frac{\dot{W}_{cv}}{\dot{m}} - \frac{\dot{Q}_{cv}}{\dot{m}} = h_1 - h_2 \qquad (1)$$

h is the specific enthalpy of the gas. A reasonable first approximation for the compressor work is:

$$\frac{\dot{W}}{\dot{m}} = c_p T_1 \left(\left(\frac{p_2}{p_1} \right)^{\frac{\gamma-1}{\eta_{pol}\gamma}} - 1 \right) \qquad (2)$$

where the polytropic efficiency, η_{pol}, is added to account for irreversibilities and heat transfer. Similarly the work available per unit mass from an expansion is;

$$\frac{\dot{W}}{\dot{m}} = c_p T_1 \left(\left(\frac{p_2}{p_1} \right)^{\frac{\eta_{pol}(\gamma-1)}{\gamma}} - 1 \right) \qquad (3)$$

The temperature of the gas is then given by;

$$T_2 = T_1 \times \left(\frac{p_2}{p_1} \right)^{\frac{\gamma-1}{\eta_{pol}\gamma}} \quad \text{For a compression}$$
$$= T_1 \times \left(\frac{p_2}{p_1} \right)^{\frac{\eta_{pol}(\gamma-1)}{\gamma}} \quad \text{For an expansion} \qquad (4)$$

γ is the ratio of specific heats ($=c_p/c_v$) and η_{pol} is the polytropic efficiency of the compressor or turbine. Isentropic efficiency is a simpler way to account for irreversibilities, but it is dependent on compression ratio [34]. Hence it is erroneous to use it to compare compressions/expansions with different compression ratios. The polytropic (also known as infinitesimal stage or small-stage) efficiency doesn't depend on the compression ratio and thus allows for a better comparison between compressions with different pressure ratios. For example, a compression with $p_2/p_1 = 3$ and a polytropic efficiency of 85% would have an isentropic efficiency of ~82.5%, whereas $p_2/p_1 = 9$ and the same polytropic efficiency yields an isentropic efficiency of ~80%.

The exergy destruction associated with a compression or expansion is calculated by considering Equation 5 for the change in exergy in a flow stream.

$$\frac{\dot{B}}{\dot{m}} = h_2 - h_1 - T_0(s_2 - s_1) + \frac{v_2^2}{2} - \frac{v_1^2}{2} + g(z_2 - z_1) \qquad (5)$$

Here, T_0 is the ambient (dead state) temperature. Neglecting the changes in potential and kinetic energy and noting that $(h_2 - h_1)$ is the compression work, the exergy destruction in the compressor is given by the $T_0(s_2 - s_1)$ term. Using $dQ = Tds$ and integrating for an ideal gas the exergy destruction in the compressor and turbine can be calculated as:

$$\frac{\dot{B}}{\dot{m}} = T_0 \left(c_p \ln \frac{T_2}{T_1} - R \ln \frac{p_2}{p_1} \right) \qquad (6)$$

Unless the High Pressure (HP) air store is isobaric (kept at constant pressure), the states described in the Equations 2 and 3 will be constantly changing. Each increment of air, Δm, must be compressed to a pressure just above the store pressure for air to flow into the store. Therefore, the final pressure p_2 of the compression will increase as the pressure in the store increases from the initial storage pressure to the maximum storage pressure $p_{store,max}$, and during expansion the initial pressure p_1 will fall as the pressure inside the store decreases.

In order to model the compression phase we use a *finite* step approach. The model considers an increment of air, Δm, which is compressed from the ambient pressure to a pressure above the storage pressure (so that air flows into the store). The store pressure is a function of the mass of air contained within the store, hence $p_{store} = p_{store}(m)$. The work required to compress this finite amount of air, Δm, depends on how many compressions it must undergo, with the work required for the last compression given by:

$$W_{\Delta m} = \Delta m c_p T_1 \left(\left(\frac{p_{store}(m + \Delta m) + p_{loss}}{p_1} \right)^{\frac{\gamma-1}{\eta_{pol,comp}\gamma}} - 1 \right) \qquad (7)$$

Here, p_1 and T_1 are the respective compressor inlet pressure and temperature, p_{loss} is any pressure loss introduced before the air reaches the HP air store (by the after-cooling heat exchanger for example) and $p_{store}(m+\Delta m)$ is the storage pressure *after* Δm has been added to the HP store, $p_{store}(m+\Delta m) > p_{store}(m)$. If

Δm passes through more than one compression, then the work required for any previous compressions where the inlet and outlet pressures are constant is given by Equation 2. After being compressed and cooled the air Δm is then added to the air store at temperature T_{store} (= T_0).

Similarly during the expansion process an amount of air, Δm, is expanded from the store pressure to the ambient pressure. The work available depends on the number of expansions undergone; with the work available from the first expansion given by:

$$W_{\Delta m} = \Delta m c_p T_1 \left(\left(\frac{p_2}{p_{store}(m-\Delta m) - p_{loss}} \right)^{\frac{\eta_{pol,turb}(\gamma-1)}{\gamma}} - 1 \right) \quad (8)$$

Now, T_1 is temperature before the expansion, p_2 is the pressure after the expansion, p_{loss} is the pressure loss through the previous heat exchanger and $p_{store}(m\text{-}\Delta m)$ is the pressure when Δm has been extracted from the HP air store. To validate the numerical model and as an interesting aside the analytical solution for the work required to fill a fixed volume constant temperature air store in which the pressure depends on the mass of air contained within the store is derived for the case in which there are no inter-cooling pressure losses in the Appendix. As seen in the Appendix the model result matches the analytical solution.

2.2 Heat storage in Packed Beds

In order to avoid very high temperatures the compression is staged, with inter-cooling between each compression and after-cooling before the air enters the store to reduce the volume required for the HP air store.

There are two distinct classes of heat exchangers that could be used in an A-CAES system: These are direct-contact and indirect-contact exchangers. In indirect-contact exchangers the heat transfer occurs through a wall that separates the fluid streams, whereas in direct-contact exchangers the heat transfer occurs via direct contact between two fluid streams or between a fluid and a solid in a packed bed regenerator. Direct-contact exchangers are less common than their indirect-contact counterparts, and this is perhaps why information concerning their application in A-CAES thus far remains scarce in available literature.

Packed bed regenerators are columns of porous solid (or packed solid particulate matter with some space between the particles- this space is called void fraction, voidage or porosity). They are extensively used for many processes in the chemical and food industries, i.e. adsorption, desorption, and rectification. They can offer very high rates of heat transfer, have very good pressure and temperature tolerances and offer relatively inexpensive construction. There has been significant recent research analysing packed beds for high temperature thermal energy storage for solar applications (i.e. [35, 36]). Using packed beds in an A-CAES system would replace both the indirect-contact exchangers and the separate thermal energy stores, forgoing the need for a separate thermal fluid.

Figure 1 depicts an incremental slice of the packed bed regenerator. Equations for the temperature of the fluid and solid phases in an incremental slice of the packed bed can be expressed using the conservation of energy.

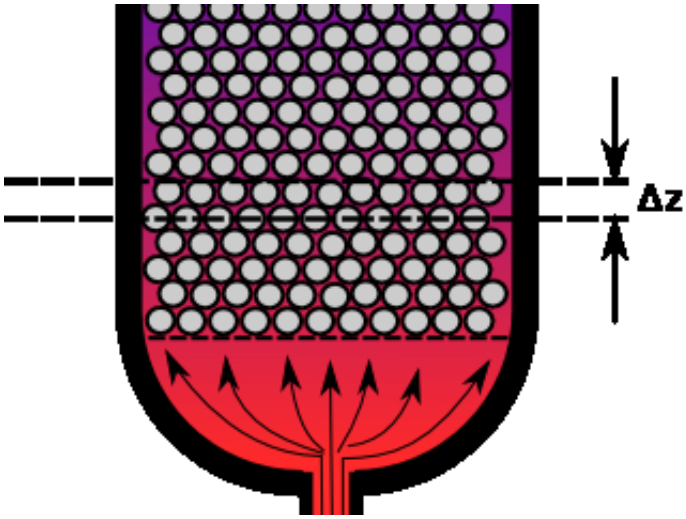

Figure 1: A depiction of a slice of height Δz in a packed bed regenerator.

Equation 9 shows the energy rate balance for the fluid phase in a slice of height Δz of the packed bed. The thermal power exchanged between the fluid and the solid phase is given by the term $\hat{h}_{vol}(T_f-T_s)\Delta z A$ while the net heat input due to the flow of the fluid is given by $v_f A \rho_f c_f (T_f(z,t)-T_f(z+\Delta z,t)) = v_f A \rho_f c_f \, dT_f/dz \, \Delta z$.

$$\varepsilon A \Delta z \rho_f c_f \frac{dT_f}{dt} = -v_f A \rho_f c_f \frac{dT_f}{dz}\Delta z - \hat{h}_{vol} A \Delta z (T_f - T_s) \quad (9)$$

The energy rate balance for the solid phase is given by Equation 10, where the term $A(d/dz)\lambda_s(dT_s/dz)$ is due to the lengthwise (in the z-direction) conduction of heat through the solid in the packed bed.

$$(1-\varepsilon)\rho_s c_s \frac{dT_s}{dt} = -\hat{h}_{vol}(T_s - T_f) - A\frac{d}{dz}\left(\lambda_s \frac{dT_s}{dz}\right) \quad (10)$$

In Equations 9 and 10 c_f and c_s are the fluid and solid specific heat capacities ($Jkg^{-1}K^{-1}$), v_f is the superficial velocity of the fluid moving through the bed (= volumetric flow rate/bed cross sectional area, ms^{-1}) and $\hat{h}_{vol}$ is the volumetric heat transfer coefficient ($Wm^{-3}K^{-1}$). The void fraction is denoted ε, hence the mass of the fluid and the solid in a slice Δz are given by Equations 11 and 12.

$$m_f = \rho_f \varepsilon A \Delta z \quad (11)$$

$$m_s = \rho_s (1-\varepsilon) A \Delta z \quad (12)$$

Conservation of mass means the rate of change of fluid density in a slice is equal to the difference between mass flow rate across the slice.

$$\frac{d\rho_f}{dt} = \frac{d(v_f \rho_f)}{dz} \quad (13)$$

Equations 9 and 10 are the standard 1-d equations for the temperature profile of a packed bed exchanger. The case in which the conduction in the solid is neglected ($\lambda_s = 0$) was first solved analytically by Schumann [37] in 1929, who solved for temperature under the assumptions that; any given solid particle has a uniform temperature at any given time; there is negligible heat conduction between the solid particles; there is negligible heat conduction among the fluid particles; the fluid

motion is uniform and only in the axial direction of the solid; and the solid has a constant void fraction (porosity) and negligible radial temperature gradient. More sophisticated analytical treatments of packed bed systems can be also be found, i.e. Villatoro *et al*. (2011) [38].

The volumetric heat transfer coefficient, $\hat{h}_{vol}$, depends on the flow properties of the fluid (air), the surface area to volume ratio of the gravel and the packing geometry of the bed. Several empirical relationships to determine $\hat{h}_{vol}$ exist, as outlined in Adeyanju and Manohar (2009) [39]. We use the empirical relationship suggested by Coutier and Farber (1982) [40] when investigating the heat transfer between gravel and air:

$$\hat{h}_{vol} = 700(G/d_p)^{0.76} \tag{14}$$

G is the core mass velocity ($kgm^{-2}s^{-1}$) of the fluid and d_p is the average particle size (m). This correlation is also used by Zanganeh *et al*. (2014) [41] to analyse a packed bed system for heat storage. The Biot number, *Bi,* gives a measure of the ratio of resistance to heat transfer via conduction to the resistance of heat transfer via convection:

$$\mathrm{Bi} = \frac{\hat{h}L_c}{\lambda_s} = \frac{\hat{h}_{vol}d_p}{2\lambda_p a_p} \tag{15}$$

L_c is the characteristic length scale for heat transfer, d_p is the particle diameter, λ_s ($=\lambda_p$) is the solid particle thermal conductivity ($Wm^{-1}K^{-1}$) and a_p is the ratio of surface area to volume. If Bi << 1, then the temperature of the particle can be approximated as uniform, for example a gravel particle diameter of 10 mm leads to a Biot number around 0.01. Hence we assume that the temperature within the solid gravel particulate is constant.

3. Details of the numerical A-CAES model with Packed Beds

The model adopts a finite step approach, considering a mass increment, Δm, of air passed through the compressors and packed beds and added to the HP air store. The inlet temperatures to the packed beds are calculated from Equation 4, and discretised Equations 9, 10 and 13 are solved for each slice of the packed beds. It should be noted that Δm changes between the compressors as the pressure and temperature profile of each packed bed changes.

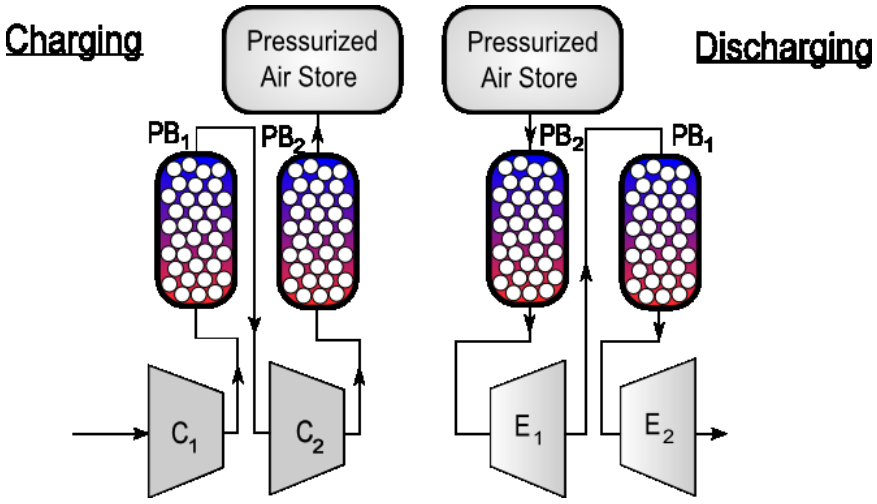

Figure 2: A schematic of an A-CAES system with packed bed heat exchangers. PB_1 provides cooling between the compressions while PB_2 cools the air entering the store. This reduces the required volume of the store.

A schematic of the model system is shown in Figure 2. The maximum storage pressure is 80 atm (8.106 MPa) and the minimum storage pressure is 20 atm (2.027 MPa). These pressures are chosen as a trade-off between minimising the range of pressures encountered and minimising the volume of the HP air store, as well as allowing the HP air store to be either a HP tank or a rock cavern. The maximum storage pressure at the McIntosh CAES facility (which uses a solution mined salt cavern) is 7.93 MPa [42].

In the model the maximum pressure ratio, r, is the same for each compression. To calculate r an estimate of the pressure loss that each cooling stage introduces is used; the pressure after the *nth* cooling stage is given by:

$$p_n = r^n p_0 - \sum_1^n r^{n-1} p_{loss} \tag{16}$$

With a final pressure of 8.106 MPa, an initial pressure of 101.3 kPa, 2 compression stages (therefore p_2=8.106 MPa) and assuming each packed bed introduces a pressure drop of 5 kPa, the pressure ratio r is 8.97. With 3 stages this decreases to 4.33. In this first analysis the intermediate expansion pressures are the same as those for the respective compression stage.

In the finite step model the solid conductivity in the lengthwise direction of the packed beds is accounted for as well as thermal power losses due to imperfect insulation of the regenerators. The insulation losses are approximated by calculating the thermal resistance of a slice of insulating cylindrical layer.

To calculate the thermal resistance we model *each slice* (as shown in Figure 1) of the packed bed as a cylinder at T_{hot} with radius r_i, contained within a hollow insulation cylinder of inner radius r_i and outer radius r_o (r_o-r$_i$ is the insulation thickness). If the heat transfer rate is slow then temperature within the insulation layer ($r_i<r<r_o$) approximately satisfies Laplace's equation. Solving this yields:

$$T = T_{hot} + \frac{T_{hot} - T_0}{\ln\left(r_i / r_o\right)} \ln\left(r / r_i\right) \tag{17}$$

Applying Fourier's heat law in integral form gives the thermal power loss and allows the thermal resistance ($\dot{Q} = (T_{hot}-T_0)/R_{th}$) to be calculated, where Δz is the height of the slice and λ is the thermal conductivity of the insulation material.

$$R_{th} = \frac{\ln\left(r_o / r_i\right)}{2\pi\Delta z\lambda} \tag{18}$$

The thermal resistance of the cylinder ends are also approximated for the end slices of the packed beds. In this way the thermal power loss is calculated for each slice of the bed in the model.

We also estimate the exergy loss associated with heat flow out of the packed bed. We assume that all of the available work (exergy) lost from the bed is transferred to the environment, at temperature T_0, and moreover we assume that work could have been generated from this heat reversibly. A more involved treatment recognises that work can only be generated irreversibly; therefore during the work generation process heat will be transferred to parts of the system other than the environment, having temperatures other than T_0. In this manner not all the exergy must be lost to the environment. A detailed explanation is available in appendix A of [43]. Under our assumptions in which all the available work is lost to the environment, the exergy loss associated with a flow of heat from temperature T to the ambient environment (with temperature T_0) is given by:

$$\dot{B}_{\text{heat loss}} = \left(1 - \frac{T_0}{T}\right)\dot{Q} \tag{19}$$

As heat flows out of the bed its temperature decreases, so Equation 19 becomes:

$$\delta B_{\text{heat loss}} = \left(1 - \frac{T_0}{T}\right)\delta Q \tag{20}$$

Assuming that the packed bed has a constant specific heat capacity, δQ can be written as $mc\delta T$ where c is the specific heat capacity of the packed bed. Integrating this to get the exergy loss associated with heat flow as the bed cools from T_1 to T_2 yields:

$$B_{\text{heat loss}} = mcT_0\left(\frac{T_1}{T_0} - \frac{T_2}{T_0} - \ln\frac{T_1}{T_2}\right) \tag{21}$$

Pressure losses in the packed beds are accounted for using the Ergun equation. The Ergun equation [44] provides one method of estimating the pressure drop through a packed bed and is generally regarded as suitable for a first estimate, providing the void fraction is in the range $0.33 < \varepsilon < 0.55$, the bed is made up of similar sized particles and the flow rates are moderate [45]. It is an empirical relationship, although du Plessis and Woudberg (2008) [46] has provided some theoretical validation. The Ergun equation states:

$$\frac{\Delta P}{L} = \frac{150\mu}{\psi^2 d_p^2}\frac{(1-\varepsilon)^2}{\varepsilon^3}v_f + \frac{1.75\rho_f}{\psi d_p}\frac{(1-\varepsilon)}{\varepsilon^3}v_f^2 \tag{22}$$

d_p is the particle diameter, ρ_f is the fluid density, v_f is the superficial bed velocity (the velocity that the fluid would have through an equivalent empty tube, given by volumetric flowrate divided by cross sectional area), μ is the dynamic viscosity of the fluid and ε is the void fraction of the packed bed. ψ is the shape factor to correct for the granitic gravel pieces not being spherical. The shape factor is defined in Equation 23. V_p is the volume of a single particle and A_p its surface area. The product (ψd_p) is the equivalent spherical particle diameter:

$$\psi = \frac{6V_p}{A_p d_p} \tag{23}$$

The overall efficiency of a single cycle is given by:

$$\eta = \frac{W_{\text{discharge}}}{W_{\text{charge}}} \tag{24}$$

where W_{charge} is the total work input required to run the compression and $W_{discharge}$ is the total useful work released by the expansion. The exergy balance for the system is given by:

$$W_{\text{charge}} = W_{\text{discharge}} + B_{\text{d,comp}} + B_{\text{d,exp}} + B_{\text{lost,exit}} + B_{\text{lost,PB}} + B_{\text{d,PB}} \tag{25}$$

$B_{d,comp}$ is the exergy destroyed in the compressor and $B_{d,exp}$ is the exergy destroyed in the expanders, which are estimated by the model using Equation 6. $B_{lost,exit}$ is the exergy remaining in the exhaust gas exiting the final expansion stage and is estimated using Equation 5 in the model. $B_{lost,PB}$ is the exergy lost from the packed beds as heat, including heat remaining in the beds after the cycle has finished, estimated using Equation 21. Finally $B_{d,PB}$ is the exergy destroyed in the packed from pressure losses and lengthwise conduction of heat along the bed and accounts for the remainder of the charge work.

3.1 Model Specifics

- The polytropic efficiencies of the expanders and compressors are assumed at 85%. The turbines at the McIntosh CAES facility have isentropic efficiencies of 87.4-89.1% [18], which given that the plant has 4 stages, and a high pressure between 60 and 80 bar, suggests a polytropic efficiency of ~86%.

- Heat losses from the packed beds and the air store to the environment depend on the driving temperature difference and the insulation properties. A thermal conductivity of 0.3 $Wm^{-1}K^{-1}$ is assumed for the packed bed insulation layer, as insulation materials with this thermal conductivity are easily available (fibreglass typically has a thermal conductivity less than 0.1 $Wm^{-1}K^{-1}$), and the insulation is assigned a thickness of 0.2 m.

- The PBHE is a cylinder containing uniformly sized granitic gravel particles. The gravel particles in the packed beds have a diameter of 0.01 m, a specific heat capacity of 1 $kJkg^{-1}K^{-1}$ and the effective thermal conductivity through the bed is 4 $Wm^{-1}K^{-1}$ (the solid thermal conductivity of gravel is around 2 $Wm^{-1}K^{-1}$).

- It is assumed that the specific heat capacity of the air is constant and equal to 1.01kJK^{-1}. In the temperature range encountered the specific heat varies by <5%. We also assume that the specific heat of the gravel is constant in the encountered temperature range.

- Fluid flow is assumed uniform throughout the regenerators.

- The thermal inertia of the packed bed container is neglected.

- There is no change in volume of the solid with temperature and the fluid and solid heat capacities are constant.

- The rate of heat transfer between the fluid and the solid bed is proportional to the temperature difference between them.

- Each of the individual solid particulates have uniform temperature, i.e. Bi<<1.

- Leakage of compressed air has been neglected.

For interest and for validation the full MATLAB code for the numerical A-CAES model is available at www.energystoragesense.com/downloads [47].

4. Results

Results for the simulated 2 MWh 500 kW A-CAES system are presented. Firstly consideration is given as to the effect of the number of compression/expansion stages. Secondly a single charge/discharge cycle is analysed to see where the main losses occur. Finally continuous charging and discharging is simulated to predict how the system may operate under continuous cycling.

4.1 Number of compression stages

The system depicted in Figure 2 (based on the usual A-CAES design – see [25, 26] – but replacing the indirect-contact exchangers with direct-contact regenerators) has 2 compression and expansion stages. Figure 3 shows how the volume of the high pressure air store varies as the number of compression stages is varied, for one charge/discharge cycle in which the temperature of the packed bed regenerators is initially at the ambient throughout the whole length of the bed. Although no system is anticipated to use 100 stages the extrapolation serves as a useful check to compare against isothermal operation.

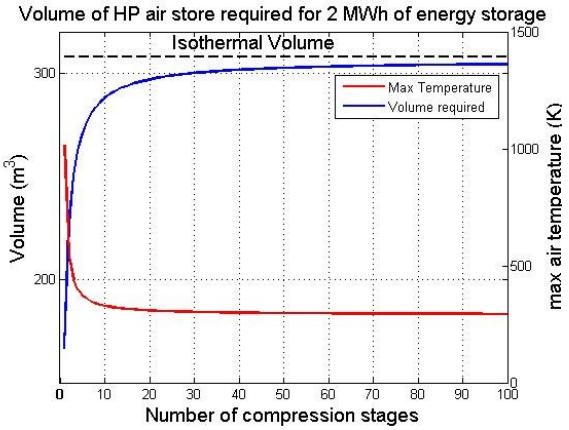

Figure 3: Graph showing how the HP (80 atm) storage volume and maximum temperature achieved in the compression depends on the number of compression stages. These results represent the initial cycle, with the regenerators starting at ambient temperature.

The energy density is decreased as the number of compression stages is increased and the HP air store must be larger to store the same amount of energy, as heat is stored in the packed beds at a lower temperature. The model is further validated by noting that as the number of stages gets very large the compression work required (and hence the volume required to store the desired amount of work) tends towards the isothermal value. This is calculated by replacing Equation 7 in the model with Equation 23 below.

$$W_{\Delta m} = \Delta m R T_1 \ln \frac{p(m+\Delta m)}{p_1} \tag{26}$$

The system temperatures achieved are of course lower with more compression stages. Packed bed regenerators will allow for higher system temperatures than conventional heat exchangers as there is no requirement for a thermal fluid which must remain liquid and stable throughout the range of temperatures encountered (as in the indirect-contact designs). However, it is unlikely that a final pressure of 80 atm will be practical in one compression stage. Hence we present results for modelled systems with 2, 3 and 4 compression stages to reach the final storage pressure, with the main focus on a 2-stage A-CAES system.

4.2 Single cycle exergy analysis

In this subsection we use the model developed to perform an exergy analysis of a single charge/discharge cycle of the 2-stage system in order to illustrate where the main exergy destruction in the system occurs. The system takes 4 hours to charge, remains idle for 10 hours and then is discharged for 4 hours. The exergy balance is given by Equation 25. Initially the temperature in both the packed beds is uniform and ambient. Figure 4 shows the results of the exergy analysis.

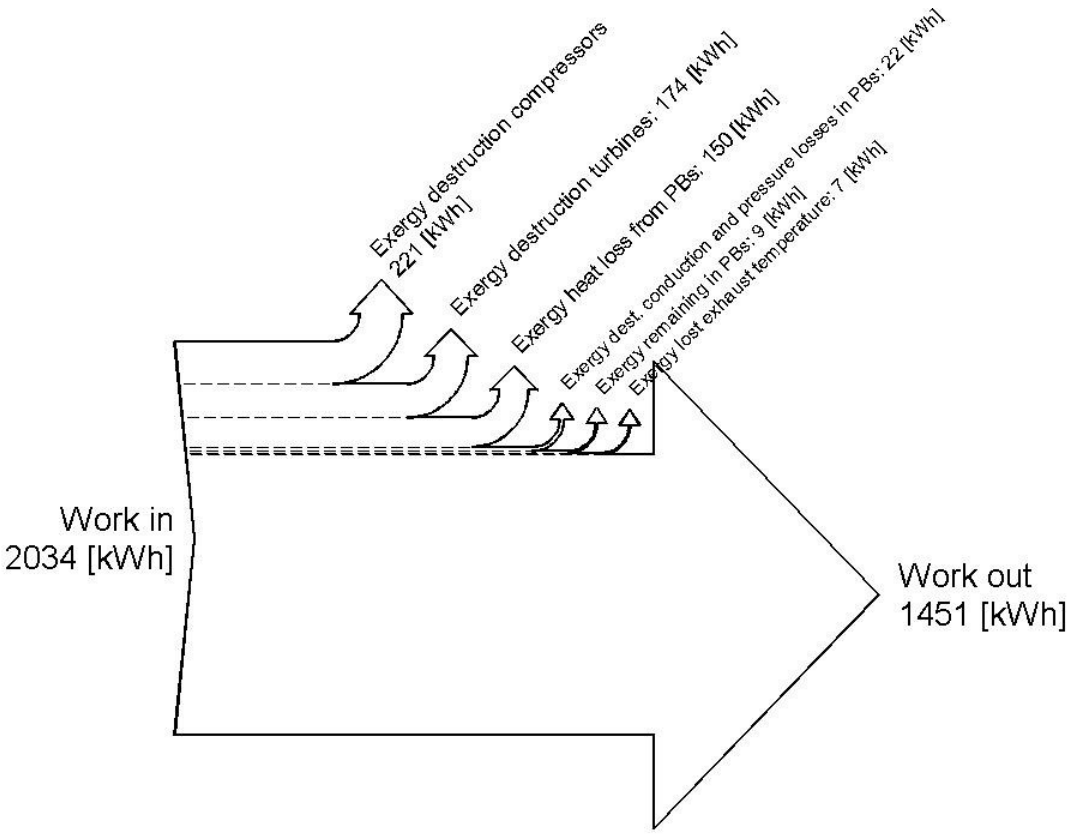

Figure 4: Results of the exergy analysis performed on the 2-stage system. Losses are ordered from largest to smallest. "Packed Beds" is abbreviated to "PBs" in the figure.

The simulated efficiency is 71.3% (obtained from Equation 24). The results show that the biggest loss (nearly 20% of the work input) occurs in the compressors and expanders. Thermal losses from the packed beds account for a further 7% of the exergy loss. Exit losses from the turbine, heat left in the packed beds, conduction losses in the packed beds and pressure losses through the packed beds make up the rest (~2%). This illustrates that maintaining high compressor and expander efficiencies throughout the system operation is the most important challenge for A-CAES. The exergy lost as heat flows from the packed bed regenerators to the surroundings is also a significant loss. This could be reduced by increasing insulation thickness; however this would increase the continuous cycling temperatures.

One particularly interesting loss is the heat that is left in the regenerators after the expansion process has been completed. This becomes particularly important when considering system operation under continuous cycling, as this heat leftover in the packed beds will affect the performance of the next cycle.

4.3 System operation under continuous cycling

As shown in [48] it is likely that any market driven energy storage system would operate over a daily cycle to exploit the daily electricity price differentials. To illustrate how the system may operate under continuous use we simulate the storage charging for 4 hours early in the morning (2am – 6am), remaining fully charged throughout the day until 4pm when it discharges until 8pm (4pm – 8pm discharging), then remaining idle until 2am and the start of the next cycle. This equates to 4 hours charging, 10 hours idle fully-charged, 4 hours discharging and then 6 hours idle empty. Thermal conduction in the packed beds and heat losses occur throughout the entire multi-cycle duration, including the idle periods. Figure 5a shows the energy stored and the energy returned over 50 successive cycles for the 2-stage system and Figure 5b shows the resulting efficiency of each cycle.

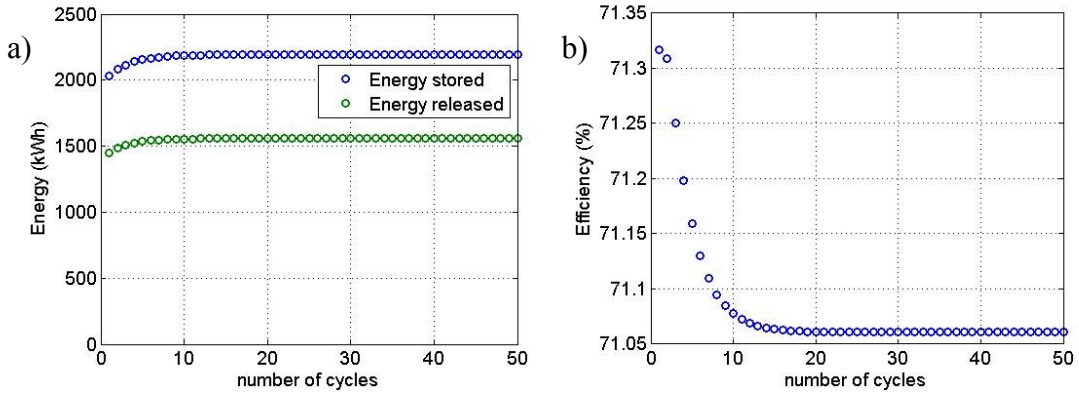

Figure 5: (a) the energy stored and the energy released over the first 50 cycles of the 2-stage system. (b) the efficiency of the first 50 cycles of the 2-stage system.

We see that transient effects mostly die out after around 20 cycles. The initial cycles are different due to differing temperature profiles in the packed beds at the start (of the cycle) – at the start of the first cycle the packed bed regenerators were at the ambient temperature throughout their length. However there are several interplaying effects that mean that the temperature profiles of the beds at the start of the next cycle are different:

1. Thermal conductivity along the length of the packed bed tends to collapse the thermal front, spreading out the heat stored in the packed bed. Therefore when the air is reheated it reaches a lower temperature and when the expansion is finished there is some heat remaining in the bed.
2. Pressure losses mean less air can be usefully removed from the HP store during discharge. The result is that not all the heat in the packed beds is used for re-heating and this (as with point 1) explains the peak in the temperature profile at the end of both of the packed beds after the discharge has finished (i.e. Figures 6a and 6g).
3. Heat loss from the beds and thermal conductivity along the beds tend to decrease the temperatures reached during discharge compared to those during charge.
4. Pressure losses result in a smaller pressure ratio during discharge (than that during charge) which tends to increase the expander outlet temperatures. Therefore the air entering the second packed bed during discharge has higher than ambient temperature (PB_1 in Figure 2) and this regenerator isn't cooled back to the ambient temperature. This effect is predominant in the early and middle part of the expansion and explains the central peak in the temperature profile of the second packed bed at the end of the discharge (Figures 6a and 6g).
5. Due to the larger heat loss from the ends of the beds (as the end of the regenerator has a higher surface-area-to-volume ratio – see Figures 6c and 6d and Figures 6e and 6f), once the thermal front gets close to the end and there is little heat left stored in the regenerator, the air exiting is heated less. This causes the first expander outlet temperature to drop towards the end of the discharge and explains why the temperature profile of the second expansion regenerator drops off after the central peak (Figures 6g and 6a).
6. During the idle time between discharge and the charge of the next cycle the temperature of the beds does tend towards the ambient, however the insulation to stop the stored compression heat escaping between charge and discharge means this process is slow, and hence the temperature profile of the regenerators doesn't change much between the discharge of the previous cycle and the charge of the next (transition from Figures 6g and 6h to 6a and 6b). The ends of the bed tend towards the ambient faster as they have a larger surface-area to volume ratio.

Figure 6 shows how the temperature profiles of the regenerators in the 2-stage system (PB_1 in Figure 2) evolve with continuous cycling. It can be seen that the temperature profile in the packed beds changes significantly compared to the initial cycle.

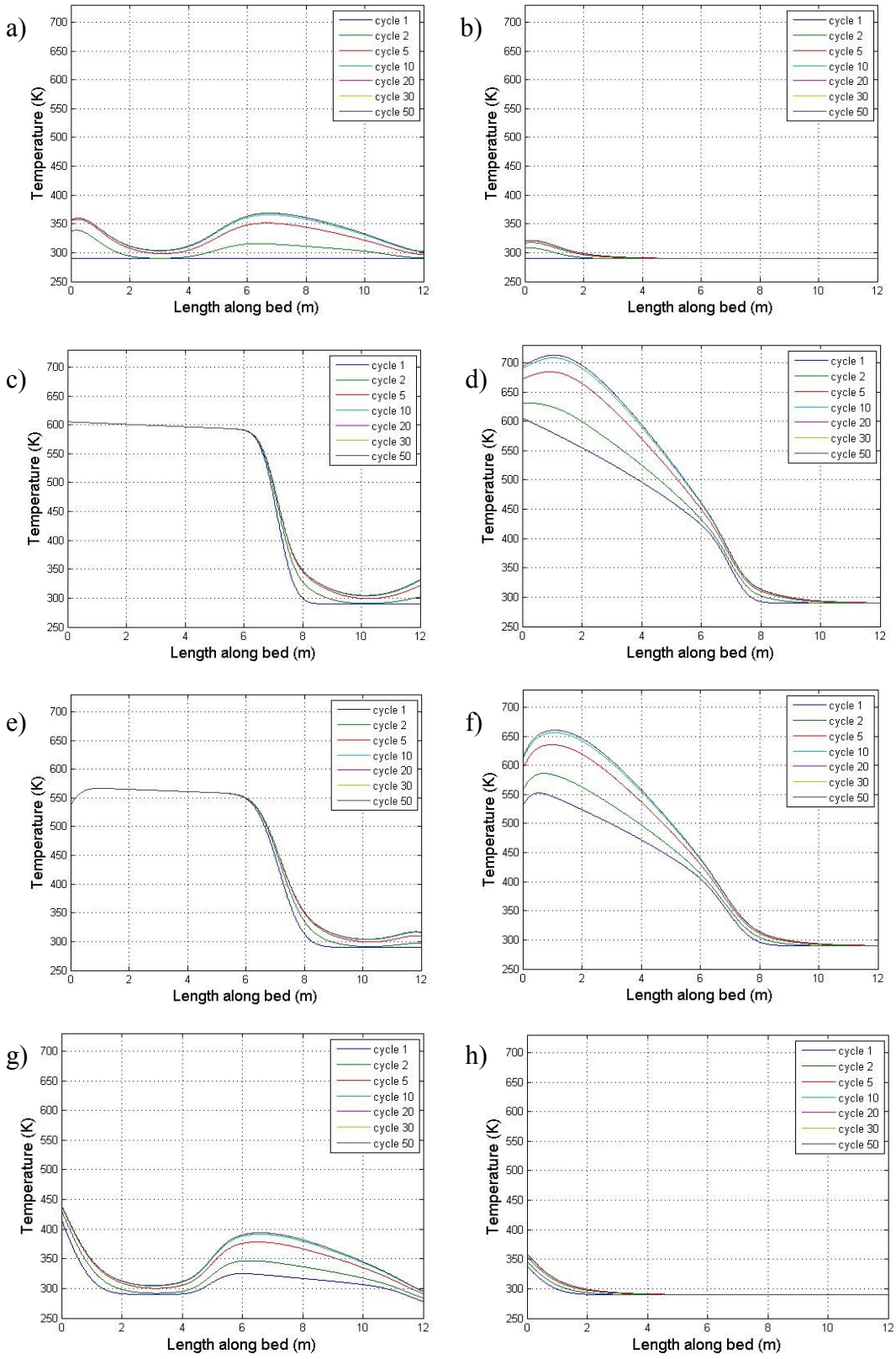

Figure 6: The figure shows the evolution of temperature profiles of the packed beds for the 2-stage system when the system is used continuously on a daily cycle with 4 hours charge, 10 hours idle, 4 hours discharge, 6 hours idle as described. (a) first packed bed at the beginning of each cycle (b) second bed at the beginning of each cycle (c) first packed bed at the end of the charge (d) second packed bed at the end of the charge (e) first packed bed at the beginning of the discharge (f) second packed bed at the beginning of the discharge (g) first packed bed at the end of the discharge (f) second packed bed at the end of the discharge.

Table 1 shows the main results of the simulations for A-CAES systems with 2 stages, 3 stages and 4 stages of compression and expansion.

	2-stage system	3-stage system	4-stage system
Charging Energy (first cycle)	2034 kWh	2033 kWh	2031 kWh
Discharging Energy (first cycle)	1451 kWh	1446 kWh	1440kWh
Charging Energy (steady state)	2193 kWh	2186 kWh	2156 kWh
Discharging Energy (steady state)	1559 kWh	1547 kWh	1520 kWh
Efficiency (first cycle)	71.3%	71.1%	70.9%
Efficiency (steady state)	71.1%	70.8%	70.5%
HP air store volume	182 m^3	204 m^3	216 m^3
Compressor/expander polytropic efficiency (isentropic efficiency will vary)	85 %	85%	85%
Max. operating pressure	80 atm (= 8.106 MPa)	80 atm (= 8.106 MPa)	80 atm (= 8.106 MPa)
Min. operating pressure	20 atm (= 2.027 MPa)	20 atm (= 2.027 MPa)	20 atm (= 2.027 MPa)
Regenerator dimensions	3 Regenerators with radius 0.6 m, length 12 m	3 Regenerators with radius 0.6 m, length 12 m	4 regenerators wwith radius 0.6 m, length 12 m
Max packed bed temperature (first cycle)	605 K	474 K	419 K
Max packed bed temperature (steady state)	713 K	556 K	469 K

Table 1: Simulations results for continuous cycling

5. Cost estimates

Costs for prototype mechanical are notoriously difficult to estimate, however a set of very simple cost estimates for the High Pressure (HP) air tank, the regenerators and the compressors and expanders is given. The HP air tank and packed beds are cost by volume of steel and the compressors and the expanders from tables of existing costs. Although these can only be regarded as "ballpark" estimates, they are useful to at least gain an order of magnitude cost for the system.

5.1 The HP air tank

Assuming the HP air tank is cylindrical, with hemispherical ends and the thickness of the walls, τ_w, is constant and much smaller than the radius ($r >> \tau_w$), the volume of material required can be approximated as:

$$V_{mat} = 2\pi r \tau_w L + 4\pi r^2 \tau_w \qquad (27)$$

where r is the internal radius and L is the length of the cylinder. The hoop stress on the cylinder walls is:

$$\chi = \frac{pr}{\tau_w} \qquad (28)$$

The ratio of the material volume to internal volume of the tank is:

$$\frac{V_{mat}}{V} = \frac{2\tau_w L + 4r\tau_w}{rL + 4r^2/3} \qquad (29)$$

Assuming a HP air store geometry in which the length is 5 times the radius ($L = 5r$), then:

$$V_{mat} = \frac{42pV}{19\chi} \quad (30)$$

Allowing a maximum steel stress of 100 MPa, the 182 m^3 HP air store (max pressure 8.106 MPa) would require ~310 tonnes of steel, assuming a density of 7800 kgm^{-3}. At $800/tonne this would cost ~$250000.

5.2 The Packed Beds

The main cost in the PBHE's will be the pressure vessel housing. We again use Equation 29 and apply the geometry specified in Table 1 to calculate the volume of material. In the 2-stage system we require that the low pressure regenerator must be able to withstand pressures up to 1 MPa, while the high pressure regenerator must withstand pressures up to 10 MPa. The LP regenerator then requires ~3 tonnes of steel while the HP requires ~25 tonnes, yielding costs of $2400 and $20000 respectively.

5.3 Compressors

The compression train is required to produce air at 80 atm, at a power of around 500 kW. Referring to page 77 of [49], delivering air at 80 atm could just be achieved using a horizontal compressor at a cost of 34.7 £/m^3h^{-1}. In terms of Free Air Delivery (FAD), the system would require about 4000 m^3h^{-1}. The total cost of the compression is then estimated at ~£140000.

5.4 Turbines

Without the ability to attain manufacturer quotes it is simply assumed that the air turbines cost will be broadly similar to the cost of the compressors. A cost of £140000 for 500 kW equates to ~440 $/kW. This is not dissimilar to costs per kW for large gas turbines (see [50]). Air turbines should also be easier to manufacture in the long term as they have only to withstand temperatures less than 1000K, as opposed to gas turbines which work with high temperatures around 2200K, and the air turbines will not have to work simultaneously with the compressors (unlike a modern gas turbine).

Summing these costs comes to ~$720k. This is anticipated to constitute the majority of the capital costs, but does not include costs for pipes, valves, the packed bed particulates, filters, pumps and insulation. Another recent article by Mignard has also attempted to estimate A-CAES costs [53].

An A-CAES system on the scale considered here will have to compete with the other storage technologies; one notable technology in the capacity and power range modelled here (2 MWh 500 kW) being NaS (Sodium Sulphur) battery systems. These systems have efficiencies in excess of 80% over the time range modelled [51]. However, with current cost estimates at 1000 – 1400 $/kWh [52] equating to $2-2.8 million for a 2 MWh NaS system, with significant operating cost and a limited cycle life it may not be unreasonable to expect that a similar size A-CAES plant will be significantly cheaper in the long term.

6. Discussions

The paper has presented a first analysis of an A-CAES system using packed bed regenerators. Despite some limitations the authors believe that the work is a useful contribution to the fields of A-CAES and energy storage. Using packed bed regenerators appears to have a number of advantages over conventional indirect-contact heat exchangers for A-CAES. Compared to a system with indirect-contact heat exchangers, the packed bed regenerator based system has no thermal fluid requirements, and hence offers a simple solution for maintaining a large degree of the temperature stratification of the thermal energy stores. This is not simply achievable using indirect-contact exchangers and a thermal fluid, as mixing of the thermal fluid would destroy stratification and results in a significantly lower efficiency, as demonstrated by the analysis of Hartmann *et al*. [30]. Packed beds should also offer higher heat transfer coefficients, have good temperature and pressure tolerances and offer simpler construction. A cost comparison between the two systems is an area of future work. The packed bed system not only removes the need for indirect-contact exchangers, thermal energy stores and a suitable

thermal fluid but also is likely to require fewer compression and expansions stages as the beds will tolerate much higher temperatures. Furthermore as there is no liquid coolant required, there is no pump required to move the thermal fluid around the system.

The simulations described in the present analysis are a simplified representation of how the real system may operate. However, even in this simple model the many different interactions lead to some complicated results – as shown by the evolution of the temperature profiles of the packed beds through successive charge/discharge cycles. Loss estimates have attempted to be conservative and it may be possible to increase performance slightly via optimisation (i.e. by optimisation of the intermediate expansion pressures). However some losses have also been omitted, i.e. leakages, pipe losses and span-wise conduction in the regenerators. Fouling and flow channelling in the regenerators may require additional filtration and a specially designed nozzle manifold for the injection of air respectively, introducing additional pressure losses. Hence the losses in the real system may also turn out to be more costly. On balance these effects are likely to have some cancellation effect.

Conventionally, compressions are designed close to isothermal to minimise the work required for a desired output pressure. However for an A-CAES system this is not necessarily the case as minimising the compression work reduces the energy density. In A-CAES the expansion process should be the exact reverse of the compression process in order to make the cycle as reversible as possible. Therefore regarding the number of stages we suggest that fewer is better, to maximise energy density, reduce pressure losses, reduce the number of components required and allow the air expanders to work with higher inlet temperatures and higher pressure ratios. It is important to realise that the systems outlined here store energy in two parts – partly in compressed gas and partly as heat; it is only the effective recombination of these parts that will lead to a successful A-CAES system. Hence another important difference with conventional compressors and those used for A-CAES is the need to store the heat of compression, so the A-CAES compressors should *minimise cooling during compression* allowing the maximum possible heat to be stored.

Accordingly it is likely that the progression of A-CAES will be aided by the development of specialised compressors designed to minimise any heat loss and output high temperature air while maximising reversibility. This equipment should be simple in that no inter-cooling will be required – however it will also need to be able to withstand higher temperatures. These compressors should provide a far better match to the reverse of modern gas turbines which operate with high pressure ratios.

7. Conclusions

We conclude that an A-CAES system based on direct-contact heat exchangers (packed beds) is a better preliminary design than a system based on indirect-contact heat exchangers. We anticipate that a continuous cycling efficiency in excess of 70% should be achievable using packed beds, as stratification of heat stored at different temperatures can be effectively preserved. In terms of efficiency the most important aspect is maintaining high compressor and expander efficiencies throughout the cycle.

A-CAES has potential as an energy storage medium. Although the work here suggests that it may struggle to match emerging battery technologies in terms of efficiency, the current high costs for battery storage, its problems with cycle life and depth of discharge, and the fact that an A-CAES system shouldn't require any exotic materials, suggest that further investigation is worthwhile.

Future detailed analysis of both packed bed and conventional heat exchanger based systems with sophisticated compression and expansion modelling would be of value, accounting for the variations in specific heat capacity and including a very rigorous packed bed model. However, should funding be available, the most informative next step may be the construction of a small-scale prototype system, developing the necessary air compression and expansion technology and comparing the use of packed beds against conventional heat exchangers.

On a final note, A-CAES is a thermo-mechanical storage system and this paper has studied its mechanical-mechanical turnaround efficiency. An alternative strategy for using A-CAES would be to use the compression heat and the cold compressed air separately, for example by using the stored heat

for hot water and the cool compressed air for simultaneous power and cooling. Investigation into this type of use is worthwhile and may turn out to have more favourable economics.

Acknowledgements

This work was supported by the Engineering and Physical Sciences Research Council under the grants EP/K002252/1 (Energy Storage for Low Carbon Grids) and EP/L014211/1 (Next Generation Grid Scale Thermal Energy Storage Technologies).

Appendix: *Validation of numerical compressor model*

This appendix derives the analytical solution for the work required to change the pressure in a constant volume constant temperature store from some initial pressure to a final pressure $p_{store,max}$ when there are no pressure losses in the after-cooling heat exchanger. The after cooling heat exchanger cools the air from the exit temperature of the compressor to the storage (= ambient) temperature. The results match the numerical model outlined by Equations 7 and 8 and so serve to provide some validation. The derivation is as follows:

Consider compressing an infinitesimal amount of gas, δm, from the ambient pressure p_0 to the storage pressure p_{store}, then cooling it back to the ambient temperature with no pressure loss, and then adding it to a store at the same temperature. Equation 2 becomes Equation A1 for an infinitesimal amount of gas.

$$\delta W = \delta m c_p T_0 \left(\left(\frac{p_{store}}{p_0} \right)^{\frac{\gamma-1}{\eta_{pol}\gamma}} - 1 \right) \quad \text{(A1)}$$

We now substitute $\delta m = M_g \, \delta n$, where n is the amount of moles compressed and M_g is the molar mass of the gas. To simplify we also substitute $x = (\gamma-1)/(\gamma\eta_{pol})$, and Equation A1 can be written as:

$$\delta W = \delta n M_g c_p T_0 \left(\left(\frac{p_{store}}{p_0} \right)^{x} - 1 \right) \quad \text{(A2)}$$

Using the ideal gas law $pV = n\overline{R}T$ (where $\overline{R}$ is the universal gas constant) and substituting $\delta n T_0 = \delta p_0 V_0 / \overline{R}$ yields:

$$\delta W = \delta p_0 \frac{M_g c_p V_0}{\overline{R}} \left(\left(\frac{p_{store}}{p_0} \right)^{x} - 1 \right) \quad \text{(A3)}$$

The store temperature T_{store} is constant and equal to the ambient temperature T_0 (which is the initial temperature of the gas) and the gas is isobarically cooled back to ambient after it is compressed. Therefore, $p_0 V_0 = p_{store} V_{store}$ and hence $\delta p_0 = \delta p_{store}(V_{store}/V_0)$. Therefore it is possible to write:

$$\delta W = \delta p_{store} \frac{c_p V_{store}}{R} \left(\left(\frac{p_{store}}{p_0} \right)^{x} - 1 \right) \quad \text{(A4)}$$

where $\overline{R}$ is replaced by the specific gas constant $R = \overline{R}/M_g$. Now the total work required to change the storage pressure p_{store} from the ambient pressure p_0 to some maximum storage pressure $p_{store,max}$ can then be found by integrating Equation A4:

$$\int \delta W = \frac{c_p V_{store}}{R} \int_{p_0}^{p_{store,\max}} \left(\left(\frac{p_{store}}{p_0} \right)^x - 1 \right) dp_{store} \qquad \text{(A5)}$$

Putting in limits of p_0 and $p_{store,max}$, and re-substituting back in $x = (\gamma-1)/(\gamma\eta_{pol})$ leads to the expression for the work required to add gas at an initial pressure p_0 and temperature T_{store} to a gas store, which is also at temperature T_{store}, in which the pressure is increased from p_0 to $p_{store,max}$:

$$W = \frac{p_{store,\max} V_{store} c_p}{R} \left[\frac{p_0}{p_{store,\max}} - 1 + \frac{\eta_{pol,c}\gamma}{\gamma - 1 + \eta_{pol,c}\gamma} \left(\frac{p_{store,\max}}{p_0} \right)^{(\gamma-1)/\eta_{pol,c}\gamma} - \frac{\eta_{pol,c}\gamma}{\gamma - 1 + \eta_{pol,c}\gamma} \left(\frac{p_0}{p_{store,\max}} \right) \right]$$

(A6)

Equation A6 agrees with the numerical prediction (Equation 7) as shown in Figure A1. The work available upon expanding the air from an ever-decreasing initial storage pressure p_{store} with a maximum value $p_{store,max}$ to a constant final ambient pressure p_0 can be found in a similar manner and is given by:

$$W = \frac{p_{store,\max} V_{store} c_p}{R} \left[\frac{\gamma}{\eta_{pol,t}(\gamma-1) - \gamma} \left(\frac{p_0}{p_{store,\max}} \right) - 1 + \frac{p_0}{p_{store,\max}} - \frac{\gamma}{\eta_{pol,t}(\gamma-1) - \gamma} \left(\frac{p_0}{p_{store,\max}} \right)^{\eta_{pol,t}(\gamma-1)/\gamma} \right]$$

(A7)

Figure A1 shows illustrates how the work required to fill a 10 m^3 container with air at 3 atm (303.975 kPa) is different when the pressure in the container varies from 1 atm to 3 atm (101.325 kPa to 303.75 kPa) (calculated by Equation A6 and shown by the lower dotted line) compared to when the pressure remains constant at 3 atm (calculated by Equation 2 and shown by the upper dotted line). It also shows the work calculated by the finite step model (Equation 7) using different mass increments of air (blue line). It can be seen that the finite step method becomes a very good approximation for the work required when using mass increments equal to or less than 10^{-2} kg. Hence a mass increment of 10^{-2} kg is used throughout for the numerical model.

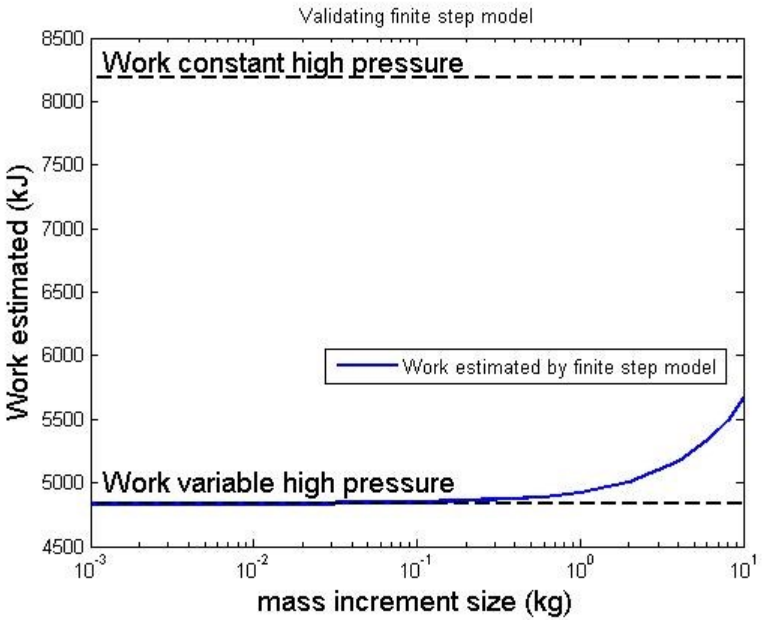

Figure A1: Illustrating the difference in the required work when the HP gas storage tank is at a constant high pressure (isobaric storage) compared to when the pressure increases as more air is added to the store (variable high pressure storage) – dotted lines. The blue line shows the numerical estimate for the variable pressure work for different mass increment sizes. A mass increment of 0.01 is used throughout for the numerical model.

References

[1] Barton JP, Infield DG. Energy storage and its use with intermittent renewable energy. Ieee T Energy Conver. 2004;19:441-8.

[2] Carrasco JM, Franquelo LG, Bialasiewicz JT, Galvan E, Guisado RCP, Prats AM, et al. Power-electronic systems for the grid integration of renewable energy sources: A survey. Ieee T Ind Electron. 2006;53:1002-16.

[3] Connolly D, Lund H, Mathiesen BV, Leahy M. The first step towards a 100% renewable energy-system for Ireland. Appl Energ. 2011;88:502-7.

[4] Lund H, Ostergaard PA, Stadler I. Towards 100% renewable energy systems. Appl Energ. 2011;88:419-21.

[5] Dell RM, Rand DAJ. Energy storage - a key technology for global energy sustainability. J Power Sources. 2001;100:2-17.

[6] Barbour E, Bryden IG. Energy storage in association with tidal current generation systems. P I Mech Eng a-J Pow. 2011;225:443-55.

[7] Duic N, Carvalho MD. Increasing renewable energy sources in island energy supply: case study Porto Santo. Renew Sust Energ Rev. 2004;8:383-99.

[8] Crotogino F, Mohmeyer K-U, Scharf R. huntorf caes: more than 20 years of successful operation. Spring 2001 Meeting, Orlando, Florida, USA, 15-18 April 20012001

[9] Nakhamkin M, Chiruvolu M. Available Compressed Air Energy Storage (CAES) Plant Concepts, 2007. 2007

[10] B.I.N.E. B.I.N.E. Informationsdienst. Projekt info 05/07, 2007. 2007.http://www.bine.info/en/publications/publikation/druckluftspeicher-kraftwerke/

[11] Cavallo A. Controllable and affordable utility-scale electricity from intermittent wind resources and compressed air energy storage (CAES). Energy. 2007;32:120-7.

[12] Greenblatt JB, Succar S, Denkenberger DC, Williams RH, Socolow RH. Baseload wind energy: modeling the competition between gas turbines and compressed air energy storage for supplemental generation. Energ Policy. 2007;35:1474-92.
[13] Lund H, Salgi G. The role of compressed air energy storage (CAES) in future sustainable energy systems. Energ Convers Manage. 2009;50:1172-9.
[14] Ibrahim H, Ilinca A, Perron J. Energy storage systems - Characteristics and comparisons. Renew Sust Energ Rev. 2008;12:1221-50.
[15] Schainker RB. Executive overview: Energy storage options for a sustainable energy future. 2004 Ieee Power Engineering Society General Meeting, Vols 1 and 2. 2004:2309-14.
[16] Schoenung SM, Eyer JM, Iannucci JJ, Horgan SA. Energy storage for a competitive power market. Annu Rev Energ Env. 1996;21:347-70.
[17] RWE power. ADELE – Adiabatic compressed air energy storage for electricity supply.http://www.rwe.com/web/cms/mediablob/en/391748/data/364260/1/rwe-power-ag/innovations/adele/Brochure-ADELE.pdf
[18] Garrison JB, Webber ME. An integrated energy storage scheme for a dispatchable solar and wind powered energy system. J Renew Sustain Ener. 2011;3.
[19] Pimm AJ, Garvey SD, de Jong M. Design and testing of Energy Bags for underwater compressed air energy storage. Energy. 2014;66:496-508.
[20] Garvey SD. The dynamics of integrated compressed air renewable energy systems. Renew Energ. 2012;39:271-92.
[21] Cheung BC, Carriveau R, Ting DSK. Parameters affecting scalable underwater compressed air energy storage. Appl Energ. 2014;134:239-47.
[22] Hydrostor.http://hydrostor.ca/home/
[23] Lightsail Energy.http://www.lightsail.com/
[24] SustainX smarter energy storage.http://www.sustainx.com/
[25] Bullough C, Gatzen C, Jakiel C, Koller M, Nowi A, Zunft S. Advanced adiabatic compressed air energy storage for the integration of wind energy. Proceedings of the European Wind Energy Conference. London2004
[26] Grazzini G, Milazzo A. Thermodynamic analysis of CAES/TES systems for renewable energy plants. Renew Energ. 2008;33:1998-2006.
[27] Pickard WF, Hansing NJ, Shen AQ. Can large-scale advanced-adiabatic compressed air energy storage be justified economically in an age of sustainable energy? J Renew Sustain Ener. 2009;1.
[28] Kim YM, Lee JH, Kim SJ, Favrat D. Potential and Evolution of Compressed Air Energy Storage: Energy and Exergy Analyses. Entropy-Switz. 2012;14:1501-21.
[29] Grazzini G, Milazzo A. A Thermodynamic Analysis of Multistage Adiabatic CAES. P Ieee. 2012;100:461-72.
[30] Hartmann N, Vohringer O, Kruck C, Eltrop L. Simulation and analysis of different adiabatic Compressed Air Energy Storage plant configurations. Appl Energ. 2012;93:541-8.
[31] Wolf D, Budt M. LTA-CAES - A low-temperature approach to Adiabatic Compressed Air Energy Storage. Appl Energ. 2014;125:158-64.
[32] Desrues T, Ruer J, Marty P, Fourmigue JF. A thermal energy storage process for large scale electric applications. Appl Therm Eng. 2010;30:425-32.
[33] White A, McTigue J, Markides C. Wave propagation and thermodynamic losses in packed-bed thermal reservoirs for energy storage. Appl Energ. 2014;130:648-57.
[34] Thomas PJ. Simulation of industrial processes for control engineers: Butterworth-Heinemann; 1999.

[35] Hanchen M, Bruckner S, Steinfeld A. High-temperature thermal storage using a packed bed of rocks - Heat transfer analysis and experimental validation. Appl Therm Eng. 2011;31:1798-806.
[36] Villatoro FR, Pérez J, Domínguez-Muñoz F, Cejudo-López JM. Approximate analytical solution for the heat transfer in packed beds for solar thermal storage in building simulators. In Eleventh International IBPSA Conference2009. p. 709-15
[37] Schumann TEW. Heat transfer: A liquid flowing through a porous prism. J Frankl Inst. 1929;208:405-16.
[38] Villatoro FR, Perez J, Santander JLG, Borovsky MA, Ratis YL, Izzheurov EA, et al. Perturbation analysis of the heat transfer in porous media with small thermal conductivity. J Math Anal Appl. 2011;374:57-70.
[39] Adeyanju AA, Manohar K. Theoretical and experimental investigation of heat transfer in packed beds. . Research Journal of Applied Sciences. 2009;4:166-7.
[40] Coutier JP, Farber EA. 2 Applications of a Numerical Approach of Heat-Transfer Process within Rock Beds. Sol Energy. 1982;29:451-62.
[41] Zanganeh G, Pedretti A, Haselbacher A, Steinfeld A. Design of packed bed thermal energy storage systems for high-temperature industrial process heat. Appl Energ. 2015;137:812-22.
[42] Nakhamkin M, Andersson L, Swensen E, Howard J, Meyer R, Schainker R, et al. Aec 110 Mw Caes Plant - Status of Project. J Eng Gas Turb Power. 1992;114:695-700.
[43] Badescu V. Optimal paths for minimizing lost available work during usual finite-time heat transfer processes. J Non-Equil Thermody. 2004;29:53-73.
[44] Ergun S. Fluid Flow through Packed Columns. Chem Eng Prog. 1952;48:89-94.
[45] Nemec D, Levec J. Flow through packed bed reactors: 1. Single-phase flow. Chem Eng Sci. 2005;60:6947-57.
[46] Du Plessis JP, Woudberg S. Pore-scale derivation of the Ergun equation to enhance its adaptability and generalization. Chem Eng Sci. 2008;63:2576-86.
[47] Barbour E.http://energystoragesense.com.
[48] Barbour E, Wilson IAG, Bryden IG, McGregor PG, Mulheran PA, Hall PJ. Towards an objective method to compare energy storage technologies: development and validation of a model to determine the upper boundary of revenue available from electrical price arbitrage. Energ Environ Sci. 2012;5:5425-36.
[49] IChemE. A Guide to Capital Cost Estimating, 3rd Edition: The Institution of Chemical Engineers, The Association of Cost Engineers.
[50] NYE Thermodynamics Corporation. Gas turbine prices.http://www.gas-turbines.com/trader/prices.htm
[51] Wen ZY, Cao JD, Gu ZH, Xu XH, Zhang FL, Lin ZX. Research on sodium sulfur battery for energy storage. Solid State Ionics. 2008;179:1697-701.
[52] Divya KC, Ostergaard J. Battery energy storage technology for power systems-An overview. Electr Pow Syst Res. 2009;79:511-20.
[53] Mignard D. Estimating the capital costs of energy storage technologies for levelling the output of renewable energy sources. Int J Environ Stud 2014;71(6):796–803